

Highly porous disk-like shape of Co_3O_4 as an anode material for lithium ion batteries

Dona Susan Baji¹ · Shantikumar V. Nair¹ · Alok Kumar Rai¹

Received: 23 March 2017 / Revised: 23 April 2017 / Accepted: 27 April 2017 / Published online: 4 May 2017
© Springer-Verlag Berlin Heidelberg 2017

Abstract A novel disk-like shape of Co_3O_4 with high porosity was synthesized by a facile hydrothermal approach followed by calcination at 485 °C for 2 h. In order to further confirm the crystal structure, morphology, particle size, surface area, and porosity of the sample, a series of corresponding characterization techniques were used. The disk-like shape of Co_3O_4 as an anode delivered excellent rate capability such as 510.5 mAh g^{-1} at 4.0 C, which is much higher than the theoretical capacity of commercial graphite anode (372 mAh g^{-1}). However, the electrode could not recover the high capacity during the long-term cycling at various higher current rates due to the deformation of the structure as confirmed by the ex situ studies. It is believed that the obtained remarkable structural feature with numerous void pores within the structure may be helpful for short-term cycling due to the large contact areas between the electrode and the electrolyte and a shorter diffusion length for lithium ion insertion but unable to act as a buffer to relax the volume expansion/contraction and alleviate the structural damage of the electrode during long-term cycling.

Keywords Co_3O_4 · Hydrothermal · Porous · Anode · Lithium ion battery

Introduction

To design new anode materials with higher safety, excellent rate performance, and great power densities, transition metal

oxides are considered as potential anodes for next-generation lithium ion battery (LIBs) [1]. Cobalt oxide (Co_3O_4) has been widely studied among all the transition metal oxides due to its high theoretical capacity (890 mAh g^{-1}), low cost, facile synthesis, and good chemical/thermal stability [2]. Since the theoretical capacity of Co_3O_4 is more than twice higher than that of commercial graphite anode (372 mAh g^{-1}), it is believed that Co_3O_4 would satisfy the requirements of future energy storage systems. However, the practical application of Co_3O_4 is still limited due to various reasons such as large volume expansion/contraction and pulverization of the electrode material during Li^+ insertion/deinsertion, which leads to cracking, fracture, and electrical contact loss of the electrode material [3]. In order to address these issues, various strategies have been attempted such as synthesis of a variety of Co_3O_4 nanostructures to increase the electrochemical activity [4], fabrication of nanocomposites with more efficient conductive components to enhance the conductivity [5], and direct growth of Co_3O_4 nanomaterials on binder-free and freestanding substrate to avoid the usage of inert components in the electrode [6]. However, in spite of all the above attempts, the issues with Co_3O_4 as an anode material are still unsolved. Therefore, in the past few years, several considerable efforts have also been made to synthesize highly porous Co_3O_4 with rationally designed novel morphologies [7, 8]. It is believed that the porous structure endows the materials with more electrochemical active sites, a large accessible surface area for the interaction with the electrolyte, and short mass/ion pathways, which were considered as potential parameters for high-performance electrode materials. However, the synthesis of the porous Co_3O_4 anode with extra accessible space for Li^+ ion insertion/extraction via a facile synthetic approach still remains a challenge.

Herein, for the first time, a facile hydrothermal approach is used to synthesize the highly porous novel disk-like shape of

✉ Alok Kumar Rai
alokkumarrail@gmail.com

¹ Amrita Centre for Nanosciences and Molecular Medicine, Amrita Vishwa Vidyapeetham, Amrita University, Kochi, Kerala 682041, India

Co_3O_4 . The obtained porous disk-like shape of the Co_3O_4 anode delivered an excellent capacity of 510.5 mAh g^{-1} at a high current rate of 4.0 C ($1 \text{ C} = 890 \text{ mA g}^{-1}$) after 50 cycles, which is still higher than the theoretical capacity of commercial graphite anode. The enhanced C-rate performance can be attributed to the highly porous unique architecture of the material in the electrode. It is believed that the porosity could increase the electrolyte/ Co_3O_4 interfacial area, shorten the Li^+ diffusion path, and improve the electrochemical kinetics. Moreover, the obtained porous structure not only provides a sufficient space to buffer against the local volume change and mitigate the pulverization problem but also promotes the easy access of the electrolyte into the bulk electrode material and offers fast lithium ion transports, which are necessary for high-rate performance.

Experimental

Material synthesis

Typically, 0.01 mol of cobalt acetate (99.999%, Sigma-Aldrich) was dissolved in a mixture of deionized water (15 ml) and ethanol (15 ml) under continuous stirring. Then, 2.5 ml of ammonium hydroxide (Nice Chemicals, India, 25%) was added dropwise to the solution to maintain the pH at 9. After continuous stirring for 1 h, the resultant solution was sealed into a Teflon-lined stainless steel autoclave and then heated at $170 \text{ }^\circ\text{C}$ for 3 h. Subsequently, the obtained material was filtered, washed with distilled water and ethanol several times, and then dried at $70 \text{ }^\circ\text{C}$ for 12 h in an oven. The as-prepared powder was eventually calcined in a muffle furnace at $485 \text{ }^\circ\text{C}$ for 2 h with a 0.25° ramp rate.

Material characterization

The crystal structure of the sample was characterized using powder X-ray diffraction (XRD, Shimadzu XRD-6000) with Cu-K_α radiation ($\lambda = 1.5406 \text{ \AA}$). Field-emission scanning electron microscopy (FE-SEM; S-4800 Hitachi) and field-emission transmission electron microscopy (FE-TEM; FEI 20 FEG) were used to examine the morphology of the sample. N_2 adsorption–desorption isotherms were measured using a BELSORP-mini II instrument. X-ray photoelectron spectroscopy (XPS) was performed using a Kratos Analytical, Ultra axis XPS instrument with a monochromatic Al K_α X-ray source. Raman spectroscopy was performed on Witec Alpha 300 RA with a diode laser as the excitation source.

Electrochemical measurements

The electrochemical tests were carried out with a CR2032-type coin cell. Lithium foil was used as the counter electrode.

The electrode slurry was made by mixing the active material, carbon black, and PVDF in a weight ratio of 70:20:10 in *N*-methyl pyrrolidone, and the resultant slurry was then uniformly pasted on a Cu foil (current collector). The electrolyte was 1 M LiPF_6 dissolved in ethylene carbonate/dimethyl carbonate mixture (1:1 in volume). The electrochemical tests were performed using BioLogic Science Instruments (BCS-805) within the voltage range of 0.01–3.0 V.

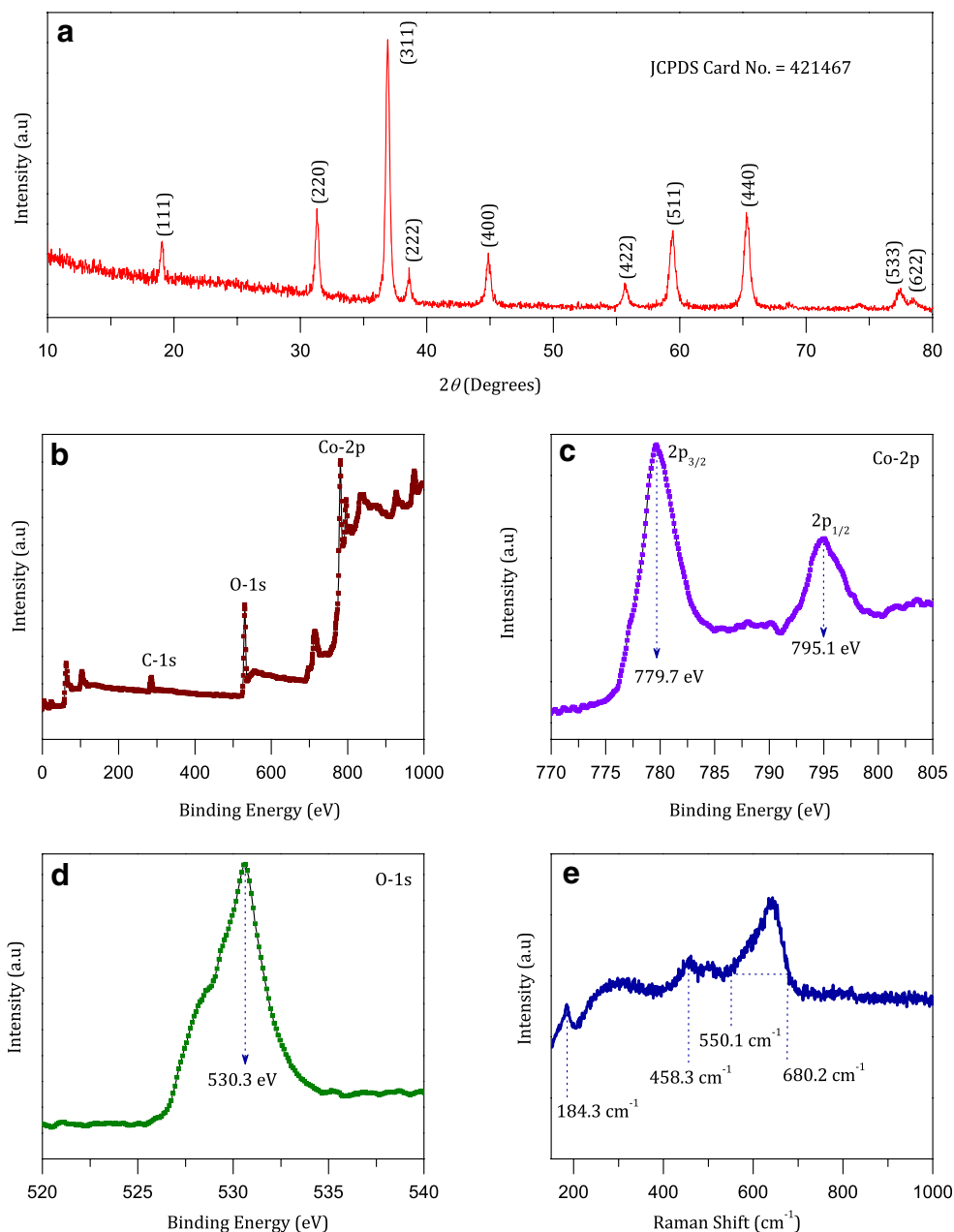
Results and discussion

Structural and morphological characterization

Figure 1a shows the XRD pattern of the annealed Co_3O_4 sample. The diffraction peaks are well-matched with that of the standard cubic spinel Co_3O_4 (JCPDS Card No. 421467). There were no other impurity peaks in the sample, indicating the phase purity of the Co_3O_4 . XPS analysis was also performed to investigate the oxidation state and surface composition of the sample. As shown in Fig. 1b, the wide spectrum of Co_3O_4 clearly shows sharp peaks of C-1s, O-1s, and Co-2p, indicating the existence of carbon, oxygen, and cobalt elements in the sample. More precisely, the high-resolution XPS spectrum of Co-2p (Fig. 1c) exhibited two peaks located at 779.7 eV for $\text{Co-2p}_{3/2}$ and 795.1 eV for $\text{Co-2p}_{1/2}$ with a binding energy difference of 15.4 eV, corresponding to the Co_3O_4 phase reported in the literature [4]. The existence of Co_3O_4 can be further confirmed by the O-1s peak (Fig. 1d) located at 530.3 eV, which corresponds to the lattice oxygen species of Co_3O_4 [4]. Figure 1e shows the Raman spectrum of the obtained Co_3O_4 sample. The sharp peaks at 184.3 and 458.3 cm^{-1} and a wide peak in the range of 550.1 to 680.2 cm^{-1} are observed, which can be attributed to the various modes of Co_3O_4 [9, 10].

Figure 2a–c shows the typical FE-SEM images of the porous disk-like shape of Co_3O_4 at different magnifications. The FE-SEM image clearly shows the disk-like shape of the sample with multi-porous structures. The dimensions of the porous Co_3O_4 structures range from ~ 500 to 1000 nm in length and ~ 700 to 900 nm in width, respectively. A detailed structural investigation of the obtained Co_3O_4 is done by HR-TEM. A high-magnification FE-TEM image of an individual Co_3O_4 structure is shown in Fig. 2d. The presence of numerous irregular pores can be observed in the structure, which is well consistent with the results of FE-SEM. The clear contrasts inside the structure also imply the presence of pores. It can be observed from the FE-TEM images (Fig. 2e, f) that the nanosized pores are uniformly distributed throughout the disk-like structures. It is reasonable to suggest that the presence of porous architecture and hollow cavities in the structure will increase the surface area of Co_3O_4 and may lead to a great enhancement of the electrochemical activities. A lattice-resolved HR-TEM study

Fig. 1 **a** XRD pattern, **b–d** XPS spectra, and **e** Raman spectra of the porous disk-like shape of Co_3O_4



of the disk-like shape of Co_3O_4 shows a well-defined crystalline structure with lattice spacing of 2.01 Å, corresponding to the (400) plane of the cubic Co_3O_4 phase. The formation of pores in the structure can be attributed to the combined effects generated by the decomposition of the large amount of organic species and the simultaneous gas evacuation during heat treatment [11, 12].

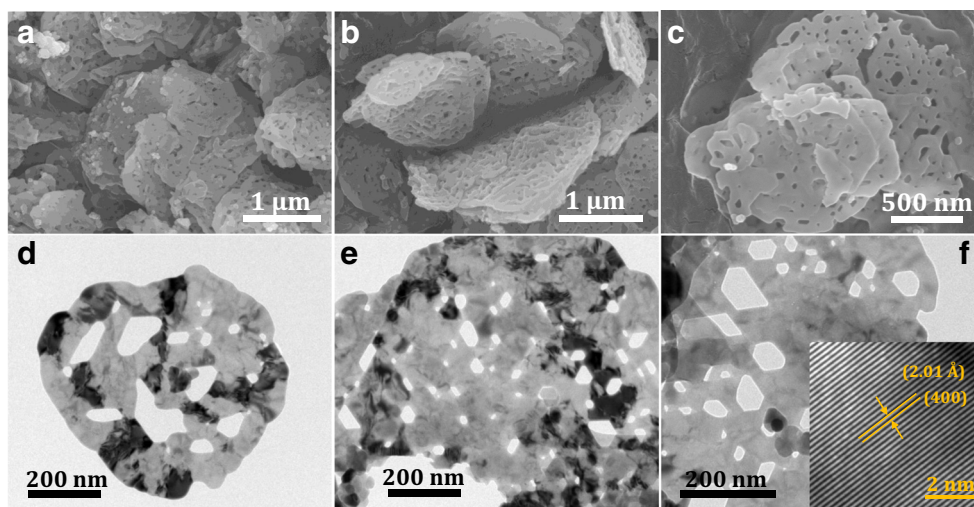
The material was further characterized by BET surface area measurement. The N_2 adsorption/desorption isotherms (Fig. 3) exhibited type IV isotherm with a H3-type hysteresis loop. The surface area of the sample was measured to be $40.4 \text{ m}^2 \text{ g}^{-1}$. The average pore diameters and pore volumes calculated by the corresponding Barrett–Joyner–Halenda

(BJH) pore size distribution curve (inset of Fig. 3) were found to be 42.5 nm and $0.43 \text{ cm}^3 \text{ g}^{-1}$, respectively, which clearly show the mesoporous nature of the disk-like shape of the Co_3O_4 sample. Obviously, the porous structure can not only provide more locations and channels for fast diffusion of Li^+ ion into the electrode material but also accommodate the volume changes of the charge/discharge process to maintain the structural integrity.

Electrochemical studies

Figure 4a displays the cyclic voltammograms (CV) for the first five cycles at a scan rate of 0.1 mV s^{-1} under the voltage

Fig. 2 a–c FE-SEM images and d–f FE-TEM images of the porous disk-like shape of Co_3O_4 at different regions. The inset of f shows the HR-TEM image of the same disk-like shape of Co_3O_4



window of 0–3.0 V. The first CV profile shows a strong cathodic peak at 0.89 V and anodic peak at 2.05 V, which can be assigned to the reversible reduction and oxidation reaction of Co_3O_4 ($\text{Co}_3\text{O}_4 + 8\text{Li}^+ + 8\text{e}^- \leftrightarrow 3\text{Co} + 4\text{Li}_2\text{O}$) along with the formation of a solid electrolyte interphase (SEI) layer [7]. The formation of the SEI layer is an irreversible process, which will result in the initial irreversible capacity loss. Afterwards, it can be seen that the anodic peak position remains the same in the subsequent cycles, whereas the cathodic peak shifts to a higher potential of 1.1 V with less intensity, which is caused by the polarization of the electrode material. After the first cycle, the overlapping of the CV curves can be seen, indicating the good reversibility of the porous disk-like shape of Co_3O_4 electrode.

Figure 4b shows the 1st, 2nd, 5th, 10th, 15th, and 20th charge/discharge profiles of the porous disk-like shape of the Co_3O_4 electrode at the current rate of 0.25 C. It can be seen

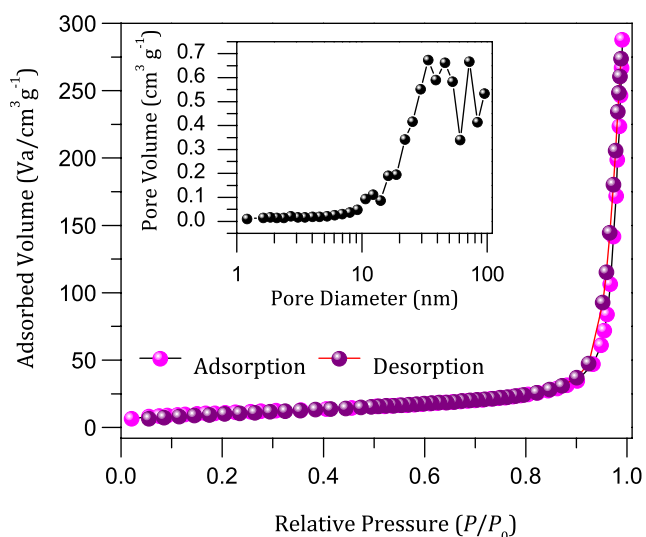


Fig. 3 Nitrogen adsorption/desorption isotherm and BJH pore size distribution curve of the porous disk-like shape of Co_3O_4

that the potential value in the first discharge curve quickly falls to 1.1 V with an extended plateau and then gradually declines to the cutoff voltage of 0.01 V, which can be assigned to the conversion reaction of Co_3O_4 to Co along with the formation of a polymer gel-like SEI layer on the surface of the Co_3O_4 particles. This finding is consistent with the above CV results. In the first cycle, the electrode delivered a discharge capacity of 1260 mAh g^{-1} and a charge capacity of 981.4 mAh g^{-1} with an initial irreversible capacity loss of 22%, which can be attributed to the inevitable formation of the SEI layer and decomposition of the electrolyte. The subsequent charge/discharge curves in the various cycles tend to be stable with high Coulombic efficiency and exhibit similar electrochemical behavior. The electrode delivered discharge and charge capacities of 1000 and 977.5 mAh g^{-1} for the 2nd cycle and 1070 and $1052.6 \text{ mAh g}^{-1}$ for the 20th cycle, respectively, with an average irreversible capacity loss of only 2%, which indicates high stability and excellent capacity retention of the electrode. It can also be noticed that the obtained capacities in the following cycles are quite higher than the theoretical capacity of Co_3O_4 (890 mAh g^{-1}), which is probably caused by the reversible formation/dissolution of the gel-like film originating from the kinetic activation in the electrode and contributing to an additional reversible capacity [4, 11].

Figure 4c shows the cycling performance of the electrode at different current rates of 0.25 and 1.0 C for 100 cycles. High reversible capacities of 851.2 mAh g^{-1} at 0.25 C and 448.4 mAh g^{-1} at 1.0 C are achieved after 100 charge/discharge cycles with almost 100% Coulombic efficiency. Moreover, in order to further investigate the effect of high porosity on the electrochemical performance of the disk-like shape of the Co_3O_4 electrode, the cycling performance was again examined at high current rates of 2.0 and 3.0 C for 100 cycles, as shown in Fig. 4d. The electrode exhibits reversible capacities of only 304 mAh g^{-1} at 2.0 C and 260.9 mAh g^{-1} at 3.0 C after 100 cycles. It can be clearly seen that the obtained

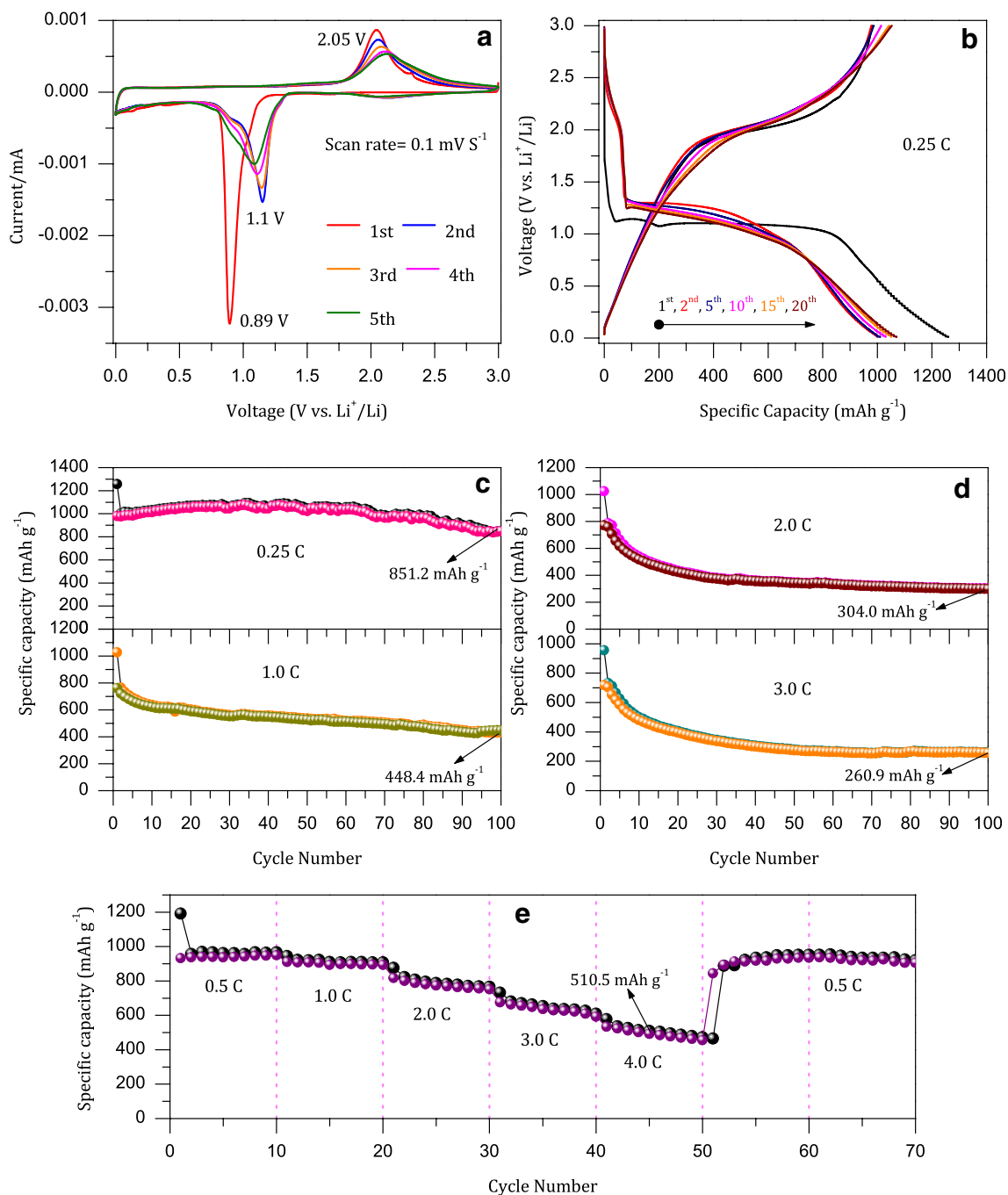


Fig. 4 a CV profile, b discharge–charge curves at 0.25 C , c cycling performance at a lower current rate of 0.25 and 1.0 C , d cycling performance at higher current rates of 2.0 and 3.0 C , e rate performance between 0.5 to 4.0 C of the porous disk-like shape of the Co_3O_4 electrode

capacities after long-term cycling on various high current rates such as 1.0 , 2.0 , and 3.0 C are not very promising towards battery application. It can also be seen that the electrode could not maintain the highest reversible capacity as obtained in the initial few cyclings during the long-term cycling. It is believed that the surface of the active material only participates in the electrochemical reaction at higher current rates due to the kinetic limitations, which leads to the decrease in the capacity

[13, 14]. In addition, it is also possible to suggest that the decrease in capacity may be due to the low electronic conductivity of Co_3O_4 since it is a semiconductor.

The rate capability of the porous disk-like shape of the Co_3O_4 electrode is also tested at various current rates between 0.5 to 4.0 C for every ten successive cycles. The C-rate profile vs. cycle number is shown in Fig. 4e, indicating that the capacity values are fairly stable at each C rate. With the

Table 1 Comparison of specific capacities of the current porous disk-like shape of the Co_3O_4 electrode with previous Co_3O_4 electrodes reported in the literatures

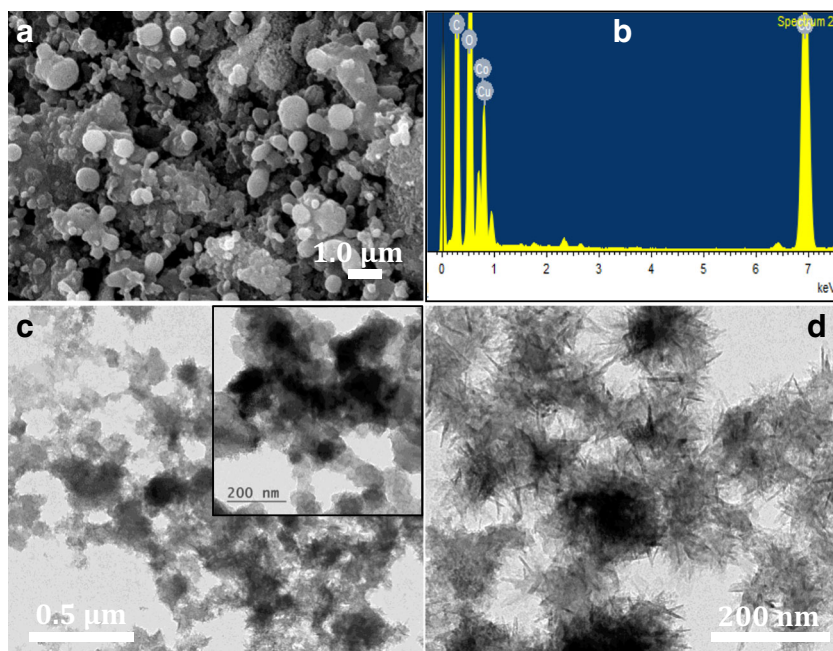
Materials	Synthesis method	Current density/rate	Cycle number	Specific capacity (mAh g^{-1})	Ref.
Co_3O_4 nanocages	Thermal decomposition	$2000 \text{ mA g}^{-1} = 2.2 \text{ C}$	25	252 mAh g^{-1}	[15]
Ultrathin mesoporous Co_3O_4 nanosheet	Hydrothermal synthesis	$2 \text{ A g}^{-1} = 2.2 \text{ C}$	50	479 mAh g^{-1}	[16]
Porous Co_3O_4 microspheres	Ultrasonic spray pyrolysis technique	$400 \text{ mA g}^{-1} = 0.45 \text{ C}$	40	654 mAh g^{-1}	[17]
Co_3O_4 cuboids	Thermolysis of metal organic framework	$1600 \text{ mA g}^{-1} = 1.8 \text{ C}$	50	163 mAh g^{-1}	[18]
Co_3O_4 mesoporous microdisks	Solvothermal synthesis	$800 \text{ mA g}^{-1} = 0.9 \text{ C}$	50	260 mAh g^{-1}	[19]
Porous Co_3O_4 nanorod	Hydrothermal synthesis	$2000 \text{ mA g}^{-1} = 2.2 \text{ C}$	25	516 mAh g^{-1}	[2]
Plate-like Co_3O_4 mesocrystal	Solution-phase route	2.0 C	40	$>500 \text{ mAh g}^{-1}$	[20]
Hierarchical network like Co_3O_4	Hydrothermal method	$1000 \text{ mA g}^{-1} = 1.1 \text{ C}$	40	31 mAh g^{-1}	[21]
Porous disk-like shape of Co_3O_4	Hydrothermal synthesis	4.0 C	50	510.5 mAh g^{-1}	Current work

increase of the current rates, the corresponding capacities were measured and found to be 964.3 mAh g^{-1} at 0.5 C , 911.2 mAh g^{-1} at 1.0 C , 788.9 mAh g^{-1} at 2.0 C , 655.2 mAh g^{-1} at 3.0 C , and 510.5 mAh g^{-1} at 4.0 C with excellent reversibility. It is worth noticing that the capacity of the electrode obtained at a high current rate of 4.0 C is still higher than the theoretical capacity of commercial graphite anode (372 mAh g^{-1}). In addition, in order to make it more clear, a comparison between the current work and various Co_3O_4 nanostructures reported in the literatures is provided in Table 1. It can be clearly seen that the porous disk-like shape of Co_3O_4 exhibits the highest capacity at 4.0 C [2, 15–21]. In addition, when the current rate returns to the initial C rate of 0.5 C after 50 cycles of charge/discharge on various high current rates, the electrode recovered almost 100% initial

capacity, which indicates the high-capacity retention capability of the electrode. It is believed that the porous architecture of the electrode could be trapping more Li^+ ions during electrochemical cycling, which leads to the improved electrochemical performance.

Ex situ studies were carried out to further understand the mechanism behind the deterioration of the capacity during long-term cycling at various higher current rates of 1.0 , 2.0 , and 3.0 C . In order to do the ex situ studies, the cycled electrodes were initially detached from the cell in an argon-filled glove box. Dimethyl carbonate was used to wash the electrode to remove the electrolyte. After drying, the electrode material was scraped off of the Cu substrate to do the ex situ SEM and TEM analyses. Figure 5a–d displays a representative ex situ SEM, EDX, and TEM of an electrode cycled at 1.0 C for 100

Fig. 5 Ex situ studies of the porous disk-like shape of the Co_3O_4 electrode cycled at 1.0 C for 100 cycles. **a** FE-SEM image, **b** EDX spectrum, **c** and **d** FE-TEM images



cycles. It can be easily observed that the porous disk-like shape of Co_3O_4 is completely deformed during cycling, indicating that the obtained highly porous disk-like shape is not capable enough to relax the volume expansion/contraction and alleviates the structural damage of the electrode during the long term cycling. However, the EDX image (Fig. 5b) clearly shows the presence of Co and O which confirmed the chemical integrity of the sample.

Conclusion

In summary, a novel disk-like shape of Co_3O_4 with high porosity was fabricated via a facile hydrothermal method. The microstructure analysis shows that the obtained Co_3O_4 is full of voids. Benefiting from this unique morphology, the disk-like shape of the Co_3O_4 anode delivered an excellent rate capability of 510.5 mAh g^{-1} at 4.0 C after 50 charge/discharge cycles with excellent reversibility. However, the electrode could not deliver the high capacity during the long-term cycling at higher current rates of 1.0, 2.0, and 3.0 C due to the deformation of the structure as confirmed by the ex situ SEM and TEM studies. The high rate capability of the electrode can be ascribed to the unique architecture of the electrode, which offers a large contact area for the electrode/electrolyte interface and short pathways for Li^+ diffusion, as well as can provide more active sites to facilitate the electrochemical reactions and increase the tolerance towards volume change.

Acknowledgements A.K. Rai is grateful to the Department of Science and technology (DST-SERB), New Delhi, Government of India, for the award of Ramanujan Fellowship (SB/S2/RJN-044/2015). This study was also supported by the Science and Engineering Research Board (SERB), Government of India, vide grant no. YSS/2015/000489.

References

- Anh LT, Rai AK, Thi TV, Gim J, Kim S, Mathew V, Kim J (2014) Enhanced electrochemical performance of novel K-doped Co_3O_4 as the anode material for secondary lithium-ion batteries. *J Mater Chem A* 2:6966–6975
- Guo J, Chen L, Zhang X, Chen H (2014) Porous Co_3O_4 nanorods as anode for lithium-ion battery with excellent electrochemical performance. *J Solid State Chem* 213:193–197
- Su Q, Zhang J, Wu Y, Du G (2014) Porous Co_3O_4 nanorods as anode for lithium-ion battery with excellent electrochemical performance. *Nano Energy* 9:264–272
- Mujtaba J, Sun H, Huang G, Molhave K, Liu Y, Zhao Y, Wang X, Xu S, Zhu J (2016) Nanoparticle decorated ultrathin porous nanosheets as hierarchical Co_3O_4 nanostructures for lithium ion battery anode materials. *Sci reports* 6:20592
- Rai AK, Gim J, Anh LT, Kim J (2013) Partially reduced Co_3O_4 /graphene nanocomposite as an anode material for secondary lithium ion battery. *Electrochim Acta* 100:63–71
- Feng K, Park HW, Wang X, Lee DU, Chen Z (2014) High performance porous anode based on template-free synthesis of Co_3O_4 nanowires for lithium-ion batteries. *Electrochim Acta* 139:145–151
- Su D, Dou S, Wang G (2014) Mesocrystal Co_3O_4 nanoplatelets as high capacity anode materials for Li-ion batteries. *Nano Res* 7:794–803
- Chen Y, Hu L (2016) Novel Co_3O_4 porous polyhedrons derived from metal-organic framework toward high performance for electrochemical energy devices. *J Solid State Chem* 239:23–29
- Kim H, Seo D, Kim S, Kim J, Kang K (2011) Highly reversible Co_3O_4 /graphene hybrid anode for lithium rechargeable batteries. *Carbon* 49:326–332
- Xiong S, Yuan C, Zhang X, Xi B, Qian Y (2009) Controllable synthesis of mesoporous Co_3O_4 nanostructures with tunable morphology for application in supercapacitors. *Chem Eur J* 15:5320–5326
- Li Z, Yu X, Paik U (2016) Facile preparation of porous Co_3O_4 nanosheets for high-performance lithium ion batteries and oxygen evolution reaction. *J Power Sources* 310:41–46
- Yuan W, Xie D, Dong Z, Su Q, Zhang J, Du G, Xu B (2013) Preparation of porous Co_3O_4 polyhedral architectures and its application as anode material in lithium-ion battery. *Mat Letters* 97:129–132
- Zaghib K, Goodenough JB, Mauger A, Julien C (2009) Unsupported claims of ultrafast charging of LiFePO_4 Li-ion batteries. *J Power Sources* 194:1021–1023
- Sahay R, Kumar PS, Aravindan V, Sundaramurthy J, Ling WC, Mhaisalkar SG, Ramakrishna S, Madhavi S (2012) High aspect ratio electrospun CuO nanofibers as anode material for lithium-ion batteries with superior cycleability. *J Phys Chem C* 116:18087–18092
- Yan N, Hu L, Li Y, Wang Y, Zhong H, Hu X, Kong X, Chen Q (2012) Co_3O_4 nanocages for high-performance anode material in lithium-ion batteries. *J Phys Chem C* 116:7227–7235
- Wu S, Xia T, Wang J, Lu F, Xu C, Zhang X, Huo L, Zhao H (2017) Ultrathin mesoporous Co_3O_4 nanosheets-constructed hierarchical clusters as high rate capability and long life anode materials for lithium-ion batteries. *Appl Surf Sci* 406:46–55
- Yin X, Wang Z, Wang J, Yan G, Xiong X, Li X, Guo H (2014) One-step facile synthesis of porous Co_3O_4 microspheres as anode materials for lithium-ion batteries. *Mat Lett* 120:73–75
- Zheng F, Yin Z, Xia H, Zhang Y (2017) MOF-derived porous Co_3O_4 cuboids with excellent performance as anode materials for lithium-ion batteries. *Mat Lett* 197:188–191
- Jin Y, Wang L, Shang Y, Gao J, Li J, He X (2015) Facile synthesis of monodisperse Co_3O_4 mesoporous microdisks as anode material for lithium ion batteries. *Electrochim Acta* 151:109–117
- Wang F, Lu C, Qin Y, Liang C, Zhao M, Yang S, Sun Z, Song X (2013) Solid state coalescence growth and electrochemical performance of plate-like Co_3O_4 mesocrystals as anode materials for lithium-ion batteries. *J Power Sources* 235:67–73
- Zhang X, Xie Q, Yue G, Zhang Y, Zhang X, Lu A, Peng D (2013) A novel hierarchical network-like Co_3O_4 anode material for lithium batteries. *Electrochim Acta* 111:746–754